17th World Conference on Earthquake Engineering, 17WCEE
Sendai, Japan - September 13th to 18th 2020

EXPERIMENTAL STUDY ON FATIGUE CHARACTERISTICS OF 780 N/mm² HIGH-STRENGTH STEEL

Y. Yaguchi [1], S. Minami [2]

[1] *Graduate Student, Tokyo Denki University, Japan, 19rmg06@ms.dendai.ac.jp*
[2] *Professor, Tokyo Denki University, Japan, minamis@g.dendai.ac.jp*

Abstract

High-strength steel of 780 N/mm^2 class has been used to both rationalize and reduce the weights of cross-sections of super high-rise and large space building structures. Such buildings are more likely to experience wind loads than seismic loads. Furthermore, safety against fatigue damage due to repeated cyclic loads has become important, in view of longer building life and long-period seismic motions.

To predict fatigue life, establishing an empirical rule called the linear cumulative fatigue damage rule (Minor's law) is recommended. In previous studies, however, fatigue experiments under two steps variable amplitude loading have been performed for various steel materials; it has been confirmed that risk exists because the application of this law is an overestimation. Additionally, reports on the fatigue of 780 N/mm^2 high-strength steel are scarce. In this study, constant amplitude fatigue loading experiments and two steps variable amplitude fatigue loading experiments were conducted to obtain basic data for the fatigue design of 780 N/mm^2 high-strength steel. Subsequently, the results were compared to the fatigue characteristics of other steel materials.

The constant amplitude fatigue loading experiments with axial strain control or load control were performed in the range of low to high cycle fatigue; fatigue life curves were obtained for each control method. In each control method, the relationship between elastic strain range $\Delta\varepsilon_e$ and cycles of fractures N_f, as well as that between plastic strain range $\Delta\varepsilon_p$ and cycles of crack initiation N_c showed a linear relationship in a double logarithmic chart. It was subsequently confirmed that the Manson–Coffin rule was established. Additionally, little difference was observed between the fatigue life curves of both methods.

In the two steps variable amplitude fatigue loading experiments, the applicability of cumulative fatigue damage D was investigated. The D–ΔN relationship revealed that the minimum value of D was approximately 0.7; hence, the application of Minor's law was confirmed to be an overestimation. Additionally, the value of ΔN when D was a minimum value tended to be larger than those of other steel materials (SS400, LY100, and SM490).

Keywords: Fatigue Life, Constant Amplitude, Manson–Coffin Rule, Two Steps Variable Amplitude, Minor's Law

1. Introduction

In recent years, high-strength steel of 780 N/mm^2 class has been increasingly used to rationalize and reduce the weights of the cross-sections of super high-rise and large space building structures. Such buildings are subjected to a large number of repeated loads due to long-period seismic motions, excellent wind loads, and longer lives of the buildings; therefore, safety against fatigue damage due to repeated cyclic loads has become important.

It is said that the prediction of fatigue life is based on an empirical rule called the linear cumulative fatigue damage rule (Minor's law), described in "Fatigue design recommendations for steel structures" by the Japanese Society of Steel Construction. In previous studies, however, fatigue experiments under two steps variable amplitude loading have been performed for various steel materials, where the cumulative fatigue damage degree D was 0.1 at the minimum. Hence, the application of this law is an overestimation. Furthermore, the relationship between the cumulative fatigue damage D and logarithmic difference of the fatigue life ΔN has been investigated. However, reports on the fatigue of 780 N/mm^2 high-strength steel is insufficient.

In this study, we conducted constant amplitude fatigue loading and two steps variable amplitude fatigue loading experiments to obtain basic data for the fatigue design of 780 N/mm^2 high-strength steel. Moreover, we compared the results with the fatigue characteristics of other steel materials from previous studies.

2. Test Specimen

The experiment was performed with a sandglass-shaped specimen of approximately 28 mm in test section length and 10 mm minimum cross-sectional diameter, as shown in Fig. 1, fabricated using 780 N/mm^2 high-strength steel. For the material tensile testing, three tensile test pieces JIS Z 2241 No.14A (with 10 mm diameter and 50 mm gauge length) were used. Table 1 shows the average values of the results of the material tensile tests, and Figs. 2 (a) and (b) show the stress–strain relationship.

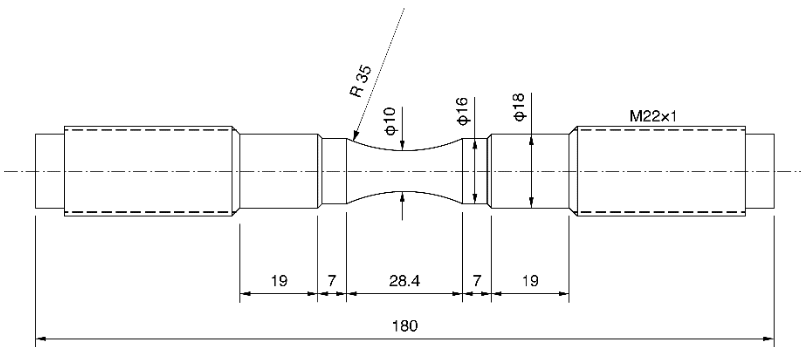

Fig. 1 – Shape of specimen

Table 1 – Material tensile test results

Young's modulus (N/mm^2)	**Proportional limit** (N/mm^2)	**0.2% Proof stress** (N/mm^2)	**Tensile strength** (N/mm^2)	**Yield ratio** (%)	**Elongation after fracture** (%)	**Reduction of aria** (%)
210,233	460	666	823	81.0	21.9	71.6

JIS Z 2241 No.14A (10 mm diameter, 50 mm gauge length)

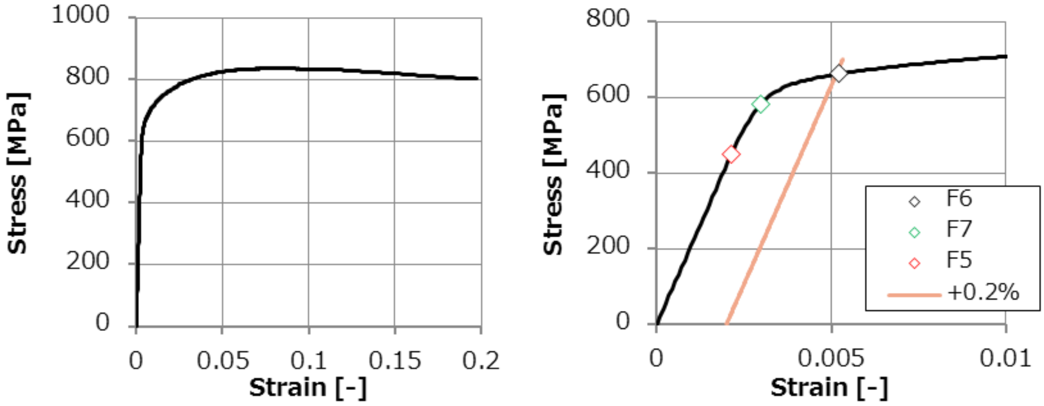

(a) Whole (b) Expansion to 1%

Fig. 2 – Stress–strain relationship

3. Experimental Method

Loading was performed with a 400 kN hydropulse fatigue testing machine, as shown in Photo 1. We conducted fatigue tests under completely reversed loading using axial strain control (strain ratio $R_\varepsilon = \varepsilon_{\max} / \varepsilon_{\min} = -1$) or load control (stress ratio $R_\sigma = \sigma_{\max} / \sigma_{\min} = -1$). Small amplitudes were used in load control, whereas large amplitudes in axial strain control, in which the diameter displacement of the minimum cross section of the specimen was detected by a diameter displacement gauge. The diameter displacements were in the thickness direction of steel. For axial strain control, the repetitive strain rate was controlled to less than 8×10^{-3}/s because a strain rate exceeding 10^{-2}/s would impose a significant effect. In all experiments, a triangular shape wave was used to maintain the strain rate. We visually observed cracks with a microscope. When a crack was discovered, the number of times to occurrences of crack N_c was determined. When the stress was reduced from the maximum value to 60% or when a specimen was broken before this point, the number of times to fracture N_f was determined We converted the load and diameter displacement into the true stress and logarithmic total strain using Eqs. (1) to (4), assuming that Hooke's law was satisfied in the elastic range and incompressibility was satisfied in the plastic range.

Photo 1 – Testing machine

$$\sigma_a = \frac{4P}{\pi d^2} \tag{1}$$

$$\varepsilon_e = \frac{\sigma_a}{E} \tag{2}$$

$$\varepsilon_p = -2\left\{\ln\left(\frac{d}{d_0}\right) + \frac{\nu\sigma_a}{E}\right\} \tag{3}$$

$$\varepsilon_a = \varepsilon_e + \varepsilon_p = -2\ln\left(\frac{d}{d_0}\right) + (1-2\nu)\cdot\frac{\sigma_a}{E} \tag{4}$$

P : Load (N)
σ_a : True stress (N/mm^2)
d_0 : Initial diameter (mm)
d : Diameter with deformation (mm)
ε_e : Axial elastic strain
ε_p : Axial logarithmic plastic strain
ε_a : Axial logarithmic total strain
ν : Poisson's ratio (= 0.3)
E : Young's modulus (= 2.05 × 10^5 N/mm^2)

3.1 Constant amplitude fatigue loading experiments

A series of experiments with axial strain control or load control was performed in the range from low cycle to high cycle fatigue, and the fatigue life curves were obtained for each control method.

The experiment with load control were performed on 12 specimens in the stress range $\Delta\sigma_a$ from 399.8 to 1513.6 N/mm^2.

In the experiment with axial strain control, the experiment was performed on four specimens, in which the axial logarithmic total strain range (hereinafter referred to as strain range) $\Delta\varepsilon_a$ was 1.33% to 9.96%.

3.2 Two steps variable amplitude fatigue loading experiments

It is assumed that fracture occurs when a certain strain amplitude $\Delta\varepsilon$ is repeated N_f times. When the strain amplitude is received once, damage is caused by 1 / N_f, and when it is received n times, the damage is n / N_f. Several $\Delta\varepsilon_i$ exist in the multistage multiple amplitude where the strain amplitude fluctuates. Each $\Delta\varepsilon_i$ damages n_i / N_{fi}. At this time, the approach in which the fracture occurs when the sum of the fatigue damage n_i / N_{fi} becomes 1 is called the linear cumulative fatigue damage rule (Minor's law), and the sum is calculated using Eq. (5) as the cumulative damage degree D.

$$D = \frac{n_1}{N_{f1}} + \frac{n_2}{N_{f2}} + \cdots + \frac{n_k}{N_{fk}} = \sum_{1}^{k} \frac{n_i}{N_{fi}} = 1 \tag{5}$$

n_i : Total number of repetitions of a certain amplitude in the two steps variable amplitude (cycles)
N_{fi} : Fatigue life at constant strain amplitude (cycles)

The effect of logarithmic difference ΔN of the fatigue life (N_H and N_L) of high and low strain amplitudes on the cumulative fatigue damage D is discussed. The logarithmic difference ΔN is defined in Eq. (6).

$$\Delta N = \log(N_L) - \log(N_H) \tag{6}$$

As shown in Fig. 3, loading started from the high amplitude side in all the specimens. The high- and low-amplitude sides were set as one block and repeated alternately until fracture. The planned value of ΔN was set from 0.5 to 2.5. The experiment was performed on five specimens.

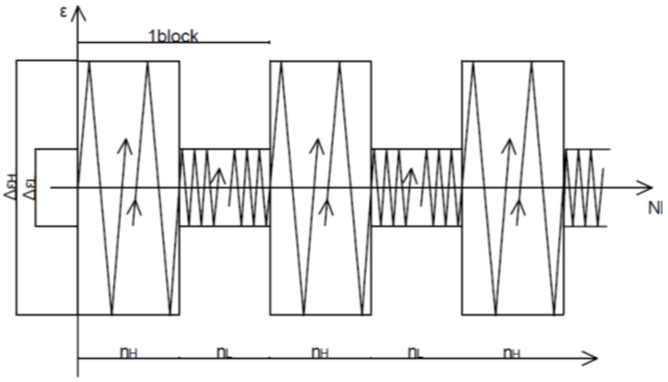

Fig. 3 – Loading program of the two steps variable amplitude

4. Experimental Results

Table 2 shows the experimental results of the constant amplitude fatigue loading experiments with load control. The loading of five specimens (CL8, CL9, CL10, CL11, and CL12) was stopped halfway because they did not break even after repeated loading exceeding 2 million cycles.

Table 2 – Experimental results of the loading control

Specimens No.	$\Delta\sigma_a$ (N/mm^2)	$\Delta\varepsilon_a$ (%)	$\Delta\varepsilon_e$ (%)	$\Delta\varepsilon_p$ (%)	N_c (cycles)	N_f (cycles)
CL1	1513.6	2.161	0.720	1.441	2.60E+2	3.45E+2
CL2	1416.7	1.203	0.674	0.529	1.14E+3	1.18E+3
CL3	1324.2	1.047	0.630	0.417	3.73E+3	3.73E+3
CL4	1161.2	0.596	0.552	0.043	2.99E+4	2.99E+4
CL5	901.5	0.429	0.429	0.000	3.08E+5	3.08E+5
CL6	860.7	0.409	0.409	0.000	6.15E+5	6.15E+5
CL7	820.0	0.390	0.390	0.000	1.94E+6	1.94E+6
CL8	799.6	0.380	0.380	0.000	>1.35E+7	>1.35E+7
CL9	763.9	0.363	0.363	0.000	>1.00E+7	>1.00E+7
CL10	720.7	0.343	0.343	0.000	>1.51E+7	>1.51E+7
CL11	601.0	0.286	0.286	0.000	>3.22E+6	>3.22E+6
CL12	399.8	0.190	0.190	0.000	>2.01E+6	>2.01E+6

The experimental results of the axial strain control are shown in Table 3. Figs. 4, 5, and 6 indicate the stress–strain relationship, stress history, and strain history of specimen CD2, respectively. A fatigue life curve for understanding the fatigue characteristics of steel materials is represented by a relationship between elastic strain range $\Delta\varepsilon_e$ and plastic strain range $\Delta\varepsilon_p$, and the cycles of repetitions N. Fig. 7 shows the fatigue life curves relating to the strain range $\Delta\varepsilon$ and cycles of crack initiation N_c, and Fig. 8 shows the fatigue life curves relating to the strain range $\Delta\varepsilon$ and cycles of fractures N_f. The relationship between the elastic strain range $\Delta\varepsilon_e$ and cycles of fractures N_f, as well as that between the plastic strain range $\Delta\varepsilon_p$ and cycles of crack initiation N_c showed a linear relationship in the double logarithmic chart. It was subsequently confirmed that the Manson–Coffin Rule was established. The regression equations based on the Manson–Coffin rule are shown in Eqs. (7) to (9) for N_c and in Eqs. (10) to (12) for N_f. Fig. 9 shows the relationship between the plastic strain range $\Delta\varepsilon_p$ and cycles of crack initiation N_c of 780 N/mm^2 high-strength steel and other steel materials (SS400, LY100, and SM490 obtained in previous studies [1 – 4]).

Table 3 – Experimental results of the axial strain control

Specimens No.	$\Delta\varepsilon_a$ (%)	$\Delta\varepsilon_e$ (%)	$\Delta\varepsilon_p$ (%)	N_c (cycles)	N_f (cycles)
CD1	9.959	0.907	9.053	17	32
CD2	4.330	0.864	3.465	70	143
CD3	2.314	0.828	1.486	250	425
CD4	1.327	0.773	0.555	1760	1899

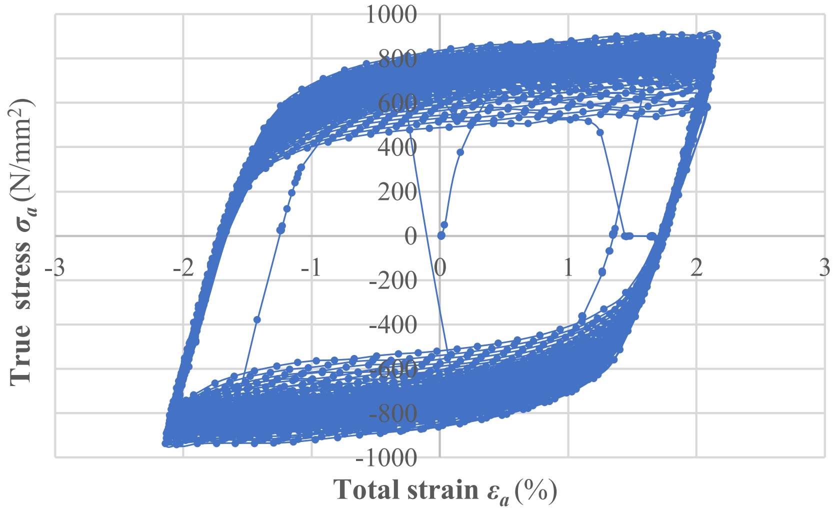

Fig. 4 – Stress–strain relationship of CD2

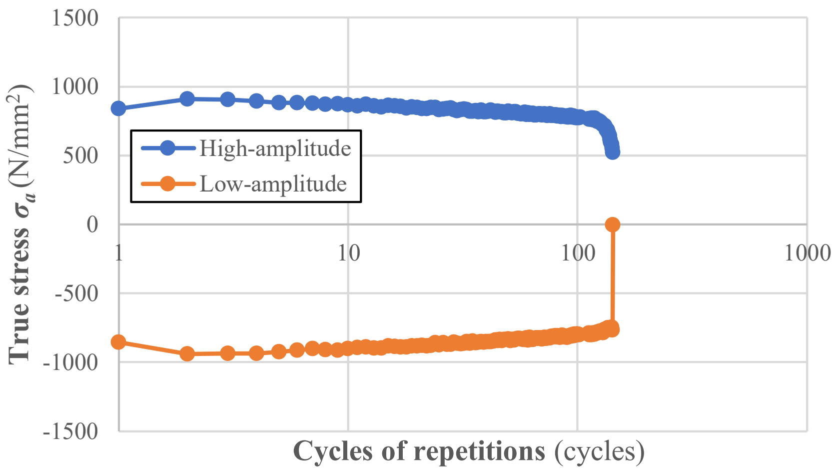

Fig. 5 – Stress history of CD2

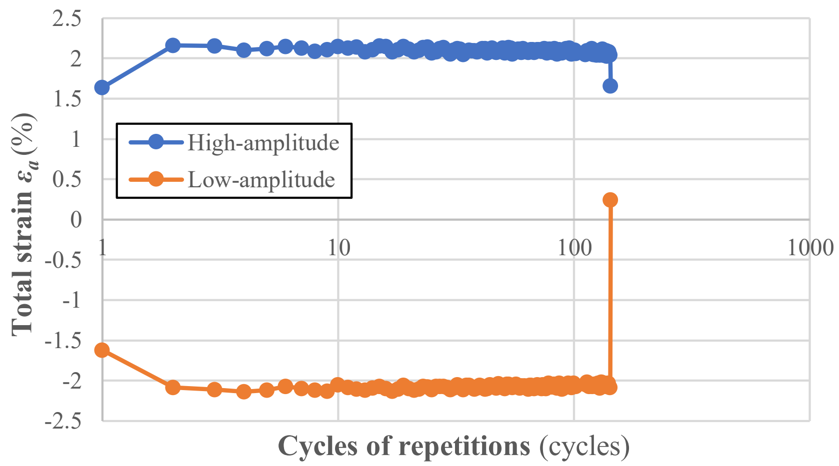

Fig. 6 – Strain history of CD2

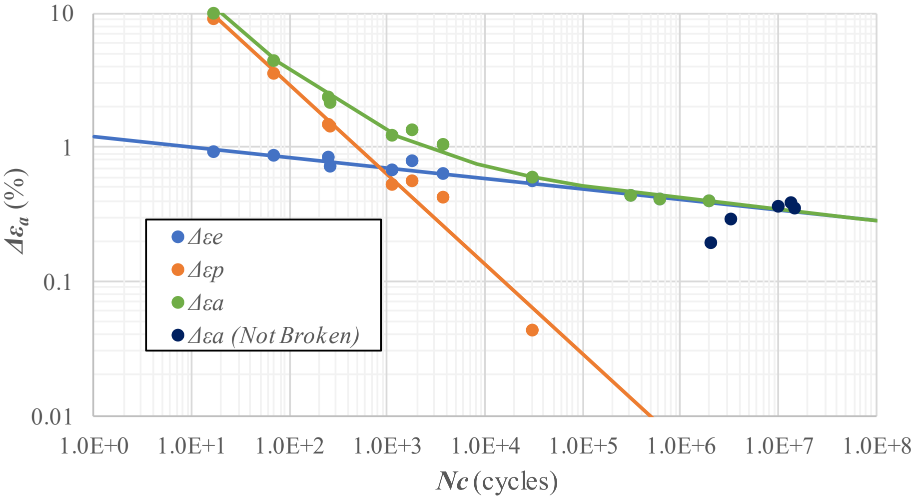

Fig. 7 – S–N curves for N_c

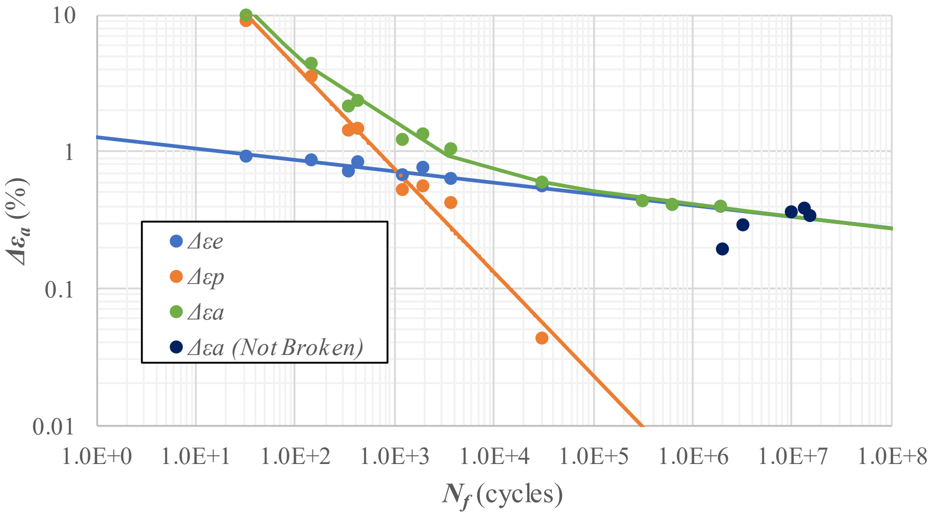

Fig. 8 – S–N curves for N_f

$$\Delta\varepsilon_e = 1.20 \times 10^{-2} N_c^{\ -0.078} \tag{7}$$

$$\Delta\varepsilon_p = 6.36 \times 10^{-1} N_c^{\ -0.669} \tag{8}$$

$$\Delta\varepsilon_a = \Delta\varepsilon_e + \Delta\varepsilon_p = 1.20 \times 10^{-2} N_c^{\ -0.078} + 6.36 \times 10^{-1} N_c^{\ -0.669} \tag{9}$$

$$\Delta\varepsilon_e = 1.27 \times 10^{-2} N_f^{\ -0.083} \tag{10}$$

$$\Delta\varepsilon_p = 1.36 N_f^{\ -0.754} \tag{11}$$

$$\Delta\varepsilon_a = \Delta\varepsilon_e + \Delta\varepsilon_p = 1.27 \times 10^{-2} N_f^{\ -0.083} + 1.36 N_f^{\ -0.754} \tag{12}$$

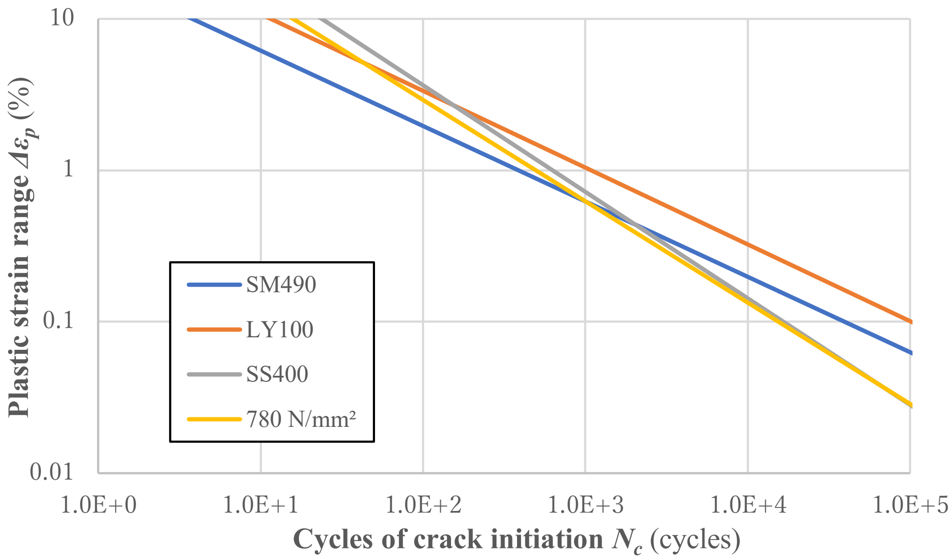

Fig. 9 – Relationship between $\Delta\varepsilon_p$ and N_c

Table 4 shows the experimental results of the two steps variable amplitude fatigue loading experiments with axial strain control. Figs. 10, 11, and 12 indicate the stress–strain relationship, stress history, and strain history of specimen TD1, respectively. In the five specimens, ΔN was between 0.41 and 2.28, and D was between 0.73 and 1.21. When ΔN was 0.41, the value of D was 1.21 of the maximum value, whereas when ΔN was 2.28, the value of D was 0.73 of the minimum value. The D–ΔN relationship in Table 4 is shown in Fig. 13 and compared with the results of previous studies [1 – 4].

Table 4 – Experimental results of two steps variable amplitude fatigue loading

Specimens No.	**Amplitude**	$\Delta\varepsilon$ (%)	N_c (cycles)	n_c (cycles)	ΔN	D
TD1	ε_H	4.355	76	58	1.55	0.95
	ε_L	0.973	2670	500		
TD2	ε_H	6.063	43	20	1.74	0.93
	ε_L	1.004	2380	1100		
TD3	ε_H	2.351	253	180	1.44	0.93
	ε_L	0.772	7000	1500		
TD4	ε_H	1.726	506	300	0.41	1.21
	ε_L	1.210	1300	800		
TD5	ε_H	6.045	43	15	2.28	0.73
	ε_L	0.749	8100	3120		

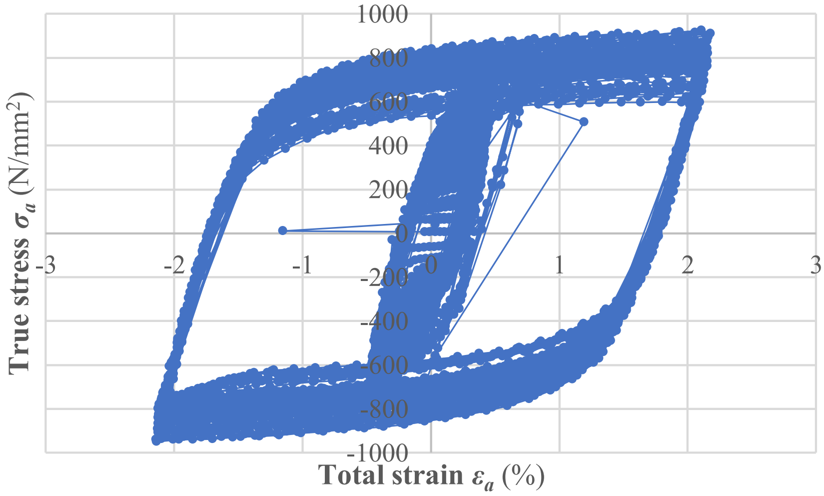

Fig. 10 – Stress–strain relationship of TD1

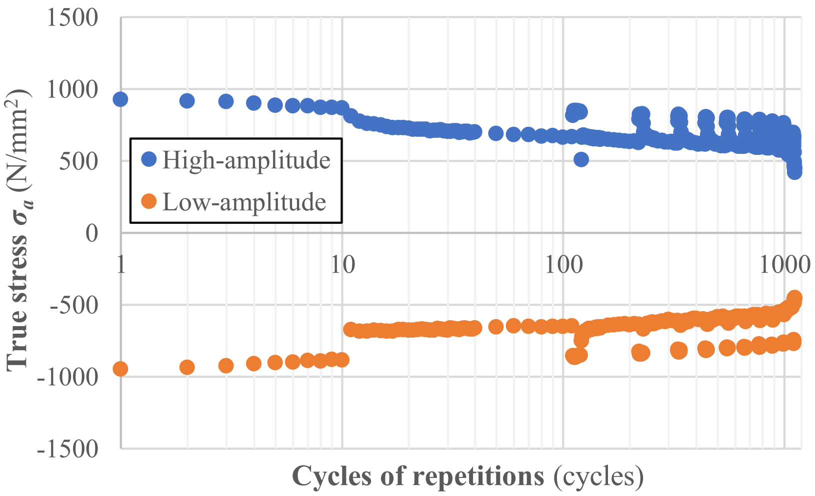

Fig. 11 – Stress history of TD1

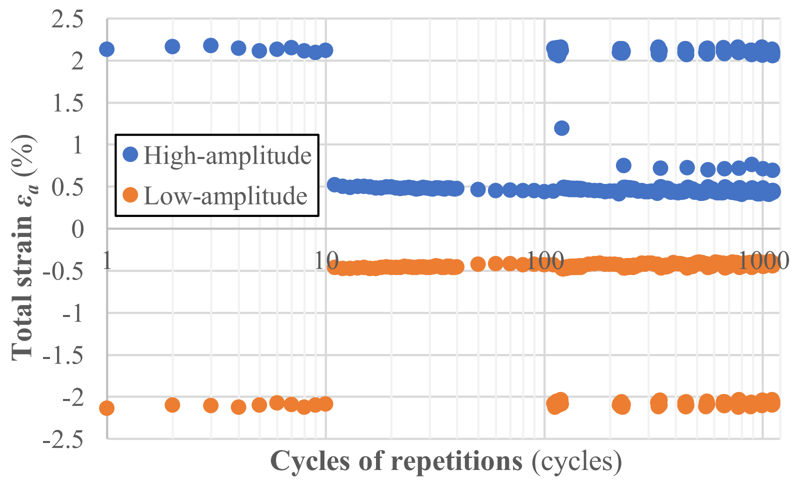

Fig. 12 – Strain history of TD1

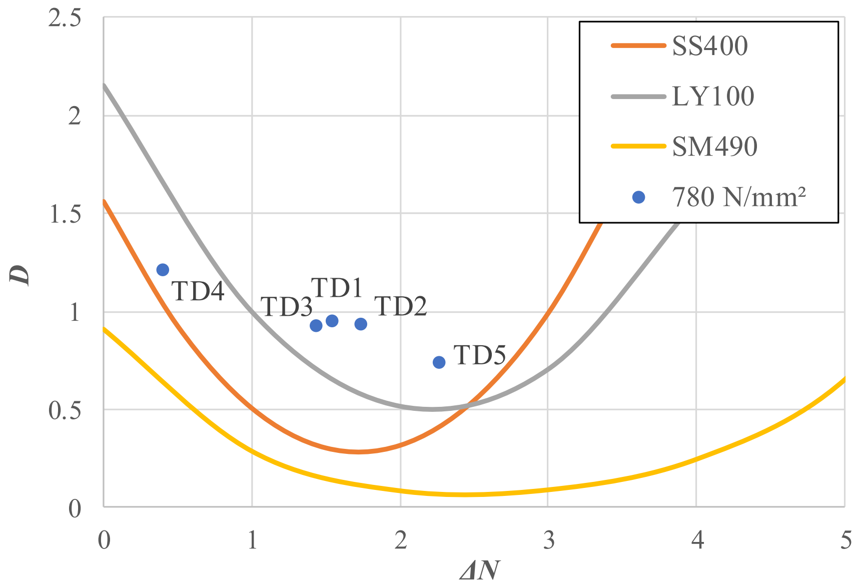

Fig. 13 – D–ΔN relationship

5. Discussion

In the constant amplitude fatigue loading experiment, the five specimens CL8, CL9, CL10, CL11, and CL12 did not break even when loading was repeated more than 2 million times. Hence, their stress ranges were considered to be below the fatigue limit; it was assumed that the fatigue limit was approximately σ_{max} = 400 N/mm^2 ($\Delta\sigma_a$ = 800 N/mm^2). As shown in Fig 9, the slope of the relationship between $\Delta\varepsilon_p$ and N_c of the 780 N/mm^2 high-strength steel is slightly gentler than that of SS400, while it is steeper than those of other steels. However, no significant difference is observed when comparing with other steel materials in terms of strain.

In the two steps variable amplitude fatigue loading experiment, from Fig. 13, D tended to decrease with the increase in ΔN. Moreover, the value of ΔN when D was a minimum value tended to be between those of SS400 and LY100. Additionally, because the D value was 0.73 when the value of D was minimum and ΔN was 2.28, the estimation of the fatigue life curve by Minor's law was overestimated. As for the cause of the shortened fatigue life, it could be assumed that cracks occurred early even at low stresses because the surface of the specimen might become uneven due to high stresses.

6. Conclusion

We obtained the following data for the fatigue design of 780 N/mm^2 high-strength steel by constant amplitude fatigue loading and two steps variable amplitude fatigue loading experiments.

1. In the constant amplitude fatigue loading experiments, not only the relationship between the plastic strain range $\Delta\varepsilon_p$ and cycles of crack initiation N_c, but also between the elastic strain range $\Delta\varepsilon_e$ and cycles of fractures N_f showed a linear relationship in the double logarithmic chart; hence, we confirmed that the Manson–Coffin rule was established.
2. The slope of the relationship between $\Delta\varepsilon_p$ and N_c of the 780 N/mm^2 high-strength steel was slightly gentler than that of SS400 but comparatively steeper than those other steels. However, no significant difference was observed when comparing with other steel materials in terms of the strain range.
3. In the two steps variable amplitude fatigue loading experiment, because the value of D was between 0.73 to 1.21, i.e., less than 1, the estimation of fatigue life using Minor's law indicated a tendency to overestimate the fatigue life, similar to other steel materials.

7. References

[1] Tadao Nakagomi, Ken Lee (1995): Experimental study on fatigue characteristic of SM490 by repeated load. *Journal of Structural and Construction Engineering*, Architectural Institute of Japan, No.469, 127-136.

[2] Yohei Seto, Tadao Nakagomi, Sunao Shiokawa (2010): Experimental study on cumulative fatigue damage of low yield point steel under two step block amplitude. *Journal of Structural and Construction Engineering*, Architectural Institute of Japan, No.653, 1265-1270.

[3] Tadao Nakagomi, Sunao Shiokawa, Ryota Wakai (2010): Experimental study on cumulative fatigue damage in low yield point steel. *Summaries of Technical Papers of Annual Meeting*, Architectural Institute of Japan, C-1, 1011-1014.

[4] Tadao Nakagomi, Haruki Kachi, Ryota Wakai (2011): Experimental study on cumulative fatigue damage in structural steel. *Summaries of Technical Papers of Annual Meeting*, Architectural Institute of Japan, C-1, 719-722.

